# Simulation-Driven Antenna Modeling by Means of Response Features and Confined Domains of Reduced Dimensionality

**ANNA PIETRENKO-DABROWSKA**[1], **(Senior Member, IEEE),**
**AND SLAWOMIR KOZIEL**[1,2], **(Senior Member, IEEE)**
[1]Faculty of Electronics, Telecommunications and Informatics, Gdańsk University of Technology, 80-233 Gdańsk, Poland
[2]Engineering Optimization & Modeling Center, Department of Technology, Reykjavik University, 101 Reykjavik, Iceland

Corresponding author: Anna Pietrenko-Dabrowska (anna.dabrowska@pg.edu.pl)

**ABSTRACT** In recent years, the employment of full-wave electromagnetic (EM) simulation tools has become imperative in the antenna design mainly for reliability reasons. While the CPU cost of a single simulation is rarely an issue, the computational overhead associated with EM-driven tasks that require massive EM analyses may become a serious bottleneck. A widely used approach to lessen this cost is the employment of surrogate models, especially data-driven ones: versatile and easily accessible. Yet, one of the unresolved issues remains the curse of dimensionality. Standard modeling techniques are merely capable of rendering surrogates for low-dimensional cases within narrow parameter ranges. In pursuit to overcome these limitations, a novel technique has been recently proposed, where the overall modeling process is carried out within a confined domain, set up based on performance specifications and spectral analysis of an auxiliary set of reference designs. This work offers a further development of the aforementioned method. Instead of tackling the entire antenna responses, only the selected characteristic points (relevant to the figures of interest considered in the antenna design process) are handled. This allows for achieving excellent model accuracy at a low computational cost. The proposed approach can be an attractive modeling alternative for systems with well-structured characteristics.

**INDEX TERMS** Antenna modeling, surrogate modeling, domain confinement, principal components, dimensionality reduction, response features.

## I. INTRODUCTION

Stringent performance requirements imposed on modern antennas, partially stemming from new emerging application areas, have led to a rapid increase in the complexity of the antenna topologies. These areas comprise, among others, wireless communications [1] (including 5G technology [2]), internet of things (IoT) [3], [4], wearable [5] or tele-medicine appliances [6]. Design of antennas for these applications requires maintaining small physical dimensions [7], [8], which makes the task even more challenging. From the utility perspective, contemporary antenna structures have to fulfill various demands, including multi-band or MIMO operation [9], [10], polarization/pattern diversity [11], [12] or

harmonic suppression [13]. To implement such functionalities, antenna geometries are gradually becoming more and more complex, and, consequently, described by an increased number of parameters. To account for the phenomena present in multi-functional antennas of reduced physical size, and/or realizing specific functions (circular polarization [14], broadband operation [15], band notches [16]), utilization of full-wave electromagnetic (EM) simulation tools is imperative. Simplified descriptions, such as analytical or equivalent networks representations, are no longer a viable option, mostly to due to their unavailability or inaccuracy.

Despite being reliable and accurate, full-wave EM simulations are computationally expensive. The aggregated simulation cost may even turn prohibitive, when repetitive analyses are required, as for common procedures such as parametric optimization [17], statistical analysis [18] or

yield estimation [19]. The expenditures boost even further in the case of global optimization procedures. In fact, performing EM-driven antenna optimization with the use of the most popular population-based metaheuristics (particle swarm [20]–[25] or genetic algorithms [26], [27]) is usually very costly. As a consequence, an extensive research effort has been directed toward expediting the optimization procedures. Miscellaneous frameworks have been developed including strictly algorithmic methods (e.g., based on selective suppression of sensitivity updates through finite differentiation [28], [29]) or the employment of adjoint sensitivities [30]. An alternative approach is to exploit surrogate models (or metamodels) [31]–[41].

One can distinguish two basic groups of metamodels, each having its advantages and drawbacks. The first one are physics-based models, which exploit the specific knowledge of the system under design, usually in the form of an underlying low-fidelity model. Among many physics-based surrogate-assisted frameworks, space mapping techniques [31], response correction algorithms [32] or adaptive response scaling [33], but also feature-based optimization [34], may be listed. Good generalization capability of the physics-based surrogates is a result of a typically high correlation between the low- and high-fidelity models. Unfortunately, in antenna design, reliable physics-based surrogates typically involve rather costly coarse-mesh EM analysis, which puts the efficacy of the overall optimization framework in question.

The second, and the most popular group of metamodels are data-driven surrogates. The primary reasons for their widespread use are the following: (i) their construction requires no physical insight; (ii) they are easily transferable between application areas, and (iii) they are readily accessible (e.g., SUMO [42], DACE [43], UQlab [44]). Plenitude of the data-driven surrogate modelling techniques have been developed, e.g., kriging [35], radial basis functions (RBF) [36], neural networks [37]–[39], Gaussian process [40] or support vector regression [41]. A primary limiting factor of data-driven models is the curse of dimensionality. In practice, constructing a reliable surrogate for modern antennas described by large numbers of parameters is hardly doable, especially when the surrogate is supposed to be valid over broad ranges of antenna operating conditions (otherwise imperative to ensure design usefulness of the model).

As a result of the aforementioned limitations, over the recent years, a class of constrained data-driven modeling techniques evolved that share a key concept of surrogate domain confinement from the standpoint of the design objectives [45]–[48]. Each of these frameworks exploits a database of high-quality designs (so-called reference points), optimized for selected operating conditions or material parameters, and serving to focus the overall modeling process in the most promising part of the parameter space. The most flexible technique of this class seems to be the nested kriging framework [47]. The technique utilizes two surrogates: the (inverse) first-level model used to define a domain for the

ultimate surrogate representing the responses of the structure under design. Due to limited amount of data available, the first-level model is a mere approximation of the manifold of optimal designs, and has to be extended in order for the surrogate model domain to comprise all designs that are optimal in a particular design context. The main benefits of the nested kriging are: (i) straightforward design of experiments, (ii) facilitated design optimization (by employing quality initial designs yielded by the first level model), (iii) low cost of setting up reliable surrogates by far surpassing that of the conventional techniques. In [48], a further advancement of nested kriging has been proposed in the form of explicit reduction of the model domain dimensionality. This is realized by performing orthogonal extension with respect to only a few selected vectors being the most dominant principal components of the reference design set. This allows for achieving a significant reduction in training data acquisition cost with respect to the basic version of the nested kriging method.

In this work, a response feature technology [49] is incorporated into the dimensionality-reduced framework [48]. More specifically, in our approach, instead of modeling the complete response of the antenna at hand, only its characteristic (feature) points are handled. This allows us to smoothen out the functional landscape to be processed, which facilitates the rendition of the surrogate model and leads to considerable reduction of the computational expenses associated with the acquisition of the training data. The actual selection of the response features is very much problem dependent. For example, in the case of multiband antennas, the natural choice may be frequency/level coordinates of their resonances or frequencies corresponding to $-10$ dB reflection levels when bandwidth manipulation is intended in the design process.

Feature-based surrogates constructed within confined domain of reduced dimensionality cover broad ranges of both the antenna parameters and the operating conditions. At the same time, the cost of the training data acquisition is a fraction of that of the conventional data-driven modelling techniques and significantly lower than for the original nested kriging framework. This is achieved at the expense of limiting the scope of applicability of the modelling method to structures whose responses feature well distinguished characteristic points, e.g., the aforementioned multi-band antennas. As a result, the proposed methodology is not as versatile as other frameworks that do not impose any restraints on the response structure of the component under design. Yet, the characteristics of many real-world antennas are inherently structured (e.g., narrow-band or multi-band antennas). Consequently, the employment of the feature-based techniques is not hindered by the aforementioned factors. Our approach is validated using a dual- and a triple-band antenna, as well as a ring-slot antenna. The surrogates obtained with the proposed technique may be successfully employed for design purposes, as it is corroborated by the provided application case studies.

The main technical contributions of the work can be summarized as follows: (i) incorporation of the response

feature technology into the performance-driven modelling framework with reduced domain dimensionality, (ii) rigorous formulation and implementation of the modelling framework, (iii) demonstration of computational benefits that can be achieved as compared to handling the complete antenna responses, (iv) demonstration of design utility of the feature-based surrogates, specifically, for reliable and rapid parameter tuning of multi-band antennas.

The remainder of the paper is structured as follows. Section II.A delineates the nested kriging modeling technique with explicit dimensionality reduction being one the main cost-reduction mechanisms of the proposed modeling framework. The second mechanism is the response feature technology described in Section II.B, whereas their incorporation into a single modeling framework is outlined in Section II.C. Section III provides verification examples corroborating suitability of the proposed methodology for antenna modeling purposes. The results are summarized in Section IV concluding the entire work.

## II. FEATURE-BASED MODELING WITHIN CONFINED DOMAIN OF REDUCED DIMENSIONALITY

This section outlines the proposed modeling framework and its three major components, i.e., performance-based domain confinement, domain dimensionality reduction using principal component analysis (PCA), and the response feature technology. The last subsection explains the incorporation of the latter into the overall modelling framework. The employment of the above listed mechanisms allows for achieving substantial savings of the training data acquisition cost in comparison to the conventional techniques. Considerable savings can be also obtained over the performance-driven modelling framework that is enhanced by the response feature technology, regardless whether the dimensionality reduction is applied or not.

Formally speaking, the problem considered in this work can be stated as follow: develop a modeling technique operating at the level of the response features and within a confined domain of reduced dimensionality to allow for rendering reliable surrogates within broad ranges of the antenna geometry parameters at the same time enabling significant lowering of the computational cost.

### A. TWO-LEVEL MODELING WITH EXPLICIT DIMENSIONALITY REDUCTION

The recently reported dimensionality-reduced performance driven modelling framework [48] follows a general paradigm of the constrained modelling [47]. In [47], the surrogate is constructed within a confined domain—a subset of the original parameter space—that encompasses high-quality designs with respect to the assumed figures of interest. The domain definition requires setting up an auxiliary inverse model (the first-level surrogate). In the original nested kriging formulation [47], it is subsequently extended in the directions orthogonal to the objective space image through the first-level model. Whereas the dimensionally-reduced domain of [48]

is defined by orthogonally extending the objective space image merely in a limited number of directions selected based on the principal component analysis of the reference design set. The volume of the confined domain (both of the original and the dimensionality-reduced one) is significantly smaller than the volume of the typically used box-constrained domain, delimited by the lower and upper bands on the design variables. This allows for constructing reliable surrogates at a fraction of the cost required by conventional modelling techniques.

### 1) REFERENCE DESIGNS PRINCIPAL COMPONENTS

In either of the constrained modelling frameworks [45]–[48], the modeling process is performed from the perspective of the objective space rather than the design space. The former is defined by the ranges on the performance figures $f_k$: $f_{k.\min} \leq f_k \leq f_{k.\max}$, $k = 1, \ldots, N$, and will be denoted as $F = [f_{1.\min} f_{1.\max}] \times \ldots \times [f_{N.\min} f_{N.\max}]$. In the case of antennas, the typical figures of interest are the operating frequencies or bandwidths, yet, they may also refer to material parameters, such as substrate permittivity. Let us also denote as $\boldsymbol{f} = [f_1 \ \ldots \ f_N]^T \in F$, the objective vector, whose entries are the performance figures $f_k$ pertinent to a particular design task. Similarly, the parameter space $X$ (i.e., the intended region of validity of the surrogate model according to the conventional modeling approach), is delimited by the ranges $l_i \leq x_i \leq u_i$, $i = 1, \ldots, n$. The vector of the antenna parameters will be denoted as $\boldsymbol{x} = [x_1 \ \ldots \ x_n]^T$, whereas $\boldsymbol{l} = [l_1 \ldots, l_n]^T$ and $\boldsymbol{u} = [u_1 \ldots, u_n]^T$, refer to the lower and upper bounds on $\boldsymbol{x}$, respectively.

The aim is to construct the surrogate within the part of the parameter space $X$ that accommodates the designs of high quality (i.e., optimum or nearly optimum for all $\boldsymbol{f} \in F$). The quality of the design $\boldsymbol{x}$ with respect to the performance figure vector $\boldsymbol{f}$ is quantified by a scalar merit function $U(\boldsymbol{x}, \boldsymbol{f})$. Thus, the design $\boldsymbol{x}^*$, optimal with respect to $\boldsymbol{f}$, is obtained by minimizing $U$ as

$$\boldsymbol{x}^* = U_F(\boldsymbol{f}) = \arg \min_{\boldsymbol{x}} U(\boldsymbol{x}, \boldsymbol{f}) \qquad (1)$$

The designs optimum in the sense of (1) for all objective vectors $\boldsymbol{f} \in F$ occupy the hypersurface $U_F(F) = \{U_F(\boldsymbol{f}): \boldsymbol{f} \in F\}$. In both the nested kriging technique [47] and PCA-based nested kriging technique [48], the surface itself was approximated with the use the reference designs $\boldsymbol{x}^{(j)} = [x_1^{(j)} \ \ldots \ x_n^{(j)}]^T$, $j = 1, \ldots, p$, rendered by optimizing the antenna in the sense of (1), where $\boldsymbol{x}^{(j)} = U_F(\boldsymbol{f}^{(j)})$ and $\boldsymbol{f}^{(j)} = [f_1^{(j)} \ \ldots \ f_N^{(j)}]$ refer to the selected target objective vectors. Clearly, uniform allocation of the vectors $\boldsymbol{f}^{(j)} = [f_1^{(j)} \ \ldots \ f_n^{(j)}]^T$, $j = 1, \ldots, p$, in $F$ is preferable to maximize the information about the structure of interest across the objective space. Often, the reference designs are rendered specifically for the purposes of the surrogate construction. Another option is the usage of the designs that have already been optimized during the previous work with the particular structure.

Clearly, a specific definition of the merit function $U(\boldsymbol{x}, \boldsymbol{f})$ is problem dependent. As an example, let us consider a multi-band antenna optimized for matching improvement at the required operating frequencies $f_{0.k}$, $k = 1, \ldots, N$. In this case the performance figures are the antenna resonant frequencies $f_k = f_{0.k}$, and a possible formulation of the merit function is

$$U(\boldsymbol{x}, \boldsymbol{f}) = \max \{|S_{11}(\boldsymbol{x}, f_{0.1})|, \ldots, |S_{11}(\boldsymbol{x}, f_{0.N})|\} \quad (2)$$

where $S_{11}(\boldsymbol{x}, f)$ stands for the antenna reflection at the design $\boldsymbol{x}$ and frequency $f$.

In this work, the surrogate domain is defined as in [48], i.e., by orthogonally extending manifold $U_F(F)$ in the most dominant directions (i.e., derived from the principal components of the reference designs). The aim is to reduce the domain dimensionality, and, thereby, to increase the prospective savings in the training data acquisition cost, without losing any important information. Through spectral decomposition of the reference design set, it is possible to gain insight into correlations between the optimum design sets and the assumed design objectives.

In the following, the basic definitions pertaining to the principal component analysis of the reference design sets are provided. Let $\boldsymbol{x}_m$ refer to a center of gravity of the set $\{\boldsymbol{x}^{(j)}\}_{j=1,\ldots,p}$

$$\boldsymbol{x}_m = \frac{1}{p} \sum_{j=1}^{p} \boldsymbol{x}^{(p)} \quad (3)$$

Further, let $\boldsymbol{S}_p$ denote the covariance matrix of $\{\boldsymbol{x}^{(j)}\}$ defined as

$$\boldsymbol{S}_p = \frac{1}{p-1} \sum_{j=1}^{p} (\boldsymbol{x}^{(j)} - \boldsymbol{x}_m)(\boldsymbol{x}^{(j)} - \boldsymbol{x}_m)^T \quad (4)$$

The principal components of the reference design set [50], i.e., the eigenvectors $\boldsymbol{a}_i$, $i = 1, \ldots, n$ of $\boldsymbol{S}_p$, indicate the most significant directions of correlations between the optimized design parameters and the target vectors within the objective space $F$. Whereas the variance of the reference set in the eigenspace is described by the eigenvalues $\lambda_i$, which are assumed to be arranged in the descending order, i.e., $\lambda_1 \geq \lambda_2 \geq \ldots \geq \lambda_n \geq 0$. We will also use the following matrix

$$\boldsymbol{A}_i = [\boldsymbol{a}_1 \ \ldots \ \boldsymbol{a}_i] \quad (5)$$

whose columns are the first $i$ eigenvectors $\boldsymbol{a}_i$. In addition, the matrix $\boldsymbol{A} = \boldsymbol{A}_n$ will stand for the matrix containing all eigenvectors.

### 2) DOMAIN DEFINITION

This subsection provides a description of the surrogate model domain definition according to the methodology proposed in [48], and adopted in this work. Toward this end, the inverse surrogate $\boldsymbol{s}_I(\boldsymbol{f}) : F \to X$, referred to as the first-level model, is rendered using the training data set $\{\boldsymbol{f}^{(j)}, \boldsymbol{x}^{(j)}\}$, $j = 1, \ldots, p$. The model $\boldsymbol{s}_I$ allows for approximating the optimum-design

surface $U_F(F)$. As the reference design set is of a limited size, $\boldsymbol{s}_I(F)$ is an imperfect rendition of $U_F(F)$. In order to accommodate the discrepancies between the two sets, $\boldsymbol{s}_I(F)$ has to be somewhat extended. In the original nested kriging formulation [47], the extension is performed in all orthogonal directions $\{\boldsymbol{v}_n^{(k)}(\boldsymbol{f})\}$, $k = 1, \ldots, n - N$, whereas in PCA-based constrained modeling [48], the extension is applied in a selective manner. Accordingly, the manifold $\boldsymbol{s}_I(F)$ is outstretched along the vectors constructed using the most dominant eigenvectors $\boldsymbol{a}_i$ of the reference set.

On the one hand, the number $K$ of the principal components, in which the extension is to be carried out, has to be greater than the number $N$ of the objectives (otherwise, the extension would be trivial). On the other hand, only the directions that carry meaningful information about the antenna response variability should be used, which is decided upon using the eigenvalue analysis. Once the exact value of $K$ is chosen the extension vectors are constructed as follows. First, the representation of $\{\boldsymbol{t}_j(\boldsymbol{f})\}_{j=1,\ldots,N}$, in the basis $\{\boldsymbol{a}_i\}_{i=1,\ldots,K}$, has to be found as

$$[\bar{\boldsymbol{t}}_1(\boldsymbol{f}) \ldots \bar{\boldsymbol{t}}_N(\boldsymbol{f})] = \boldsymbol{A}_K^T [\boldsymbol{t}_1(\boldsymbol{f}) \ldots \boldsymbol{t}_N(\boldsymbol{f})] \quad (6)$$

where $\boldsymbol{t}_j(\boldsymbol{f})$, $j = 1, \ldots, N$, denote the vectors tangent to $\boldsymbol{s}_I(F)$ at $\boldsymbol{f}$. The size of the vectors $\bar{\boldsymbol{t}}_j(\boldsymbol{f})$, $j = 1, \ldots, N$, is $K \times 1$. In finding the vectors normal to $\boldsymbol{s}_I(F)$ within the subspace spanned by the columns of the matrix $\boldsymbol{A}_K$, the following matrix $\boldsymbol{T}(\boldsymbol{f})$, being a complement of $[\bar{\boldsymbol{t}}_1(\boldsymbol{f}) \ldots \bar{\boldsymbol{t}}_N(\boldsymbol{f})]$ to a square matrix of size $K \times K$, is utilized

$$\boldsymbol{T}(\boldsymbol{f}) = [\bar{\boldsymbol{t}}_1(\boldsymbol{f}) \ \ldots \ \bar{\boldsymbol{t}}_N(\boldsymbol{f}) \ \boldsymbol{e}_{N+1} \ \boldsymbol{e}_{N+2} \ \ldots \ \boldsymbol{e}_K] \quad (7)$$

In (7), $\boldsymbol{e}_j = [0 \ \ldots \ 0 \ 1 \ 0 \ \ldots \ 0]^T$, i.e., the entries of the vector $\boldsymbol{e}_j$ are equal to zero, except for the $j$th position containing 1. Employing the Gram-Schmidt orthogonalization [51] to $\boldsymbol{T}(\boldsymbol{f})$ allows for rendering the orthonormal basis of $K$ vectors

$$\boldsymbol{T}_{GS}(\boldsymbol{f}) = [\tilde{\boldsymbol{t}}_1(\boldsymbol{f}) \ \ldots \ \tilde{\boldsymbol{t}}_N(\boldsymbol{f}) \ \boldsymbol{w}_1(\boldsymbol{f}) \ \ldots \ \boldsymbol{w}_{K-N}(\boldsymbol{f})] \quad (8)$$

The second part of the matrix $\boldsymbol{T}_{GS}$ consists of the vectors $\boldsymbol{w}_j(\boldsymbol{f})$, $j = 1, \ldots, K - N$. These will be used to extend $\boldsymbol{s}_I(F)$. The dependence of the vectors $\boldsymbol{w}_j(\boldsymbol{f})$ on the objective vector $\boldsymbol{f}$ implicates that for each $\boldsymbol{f} \in F$ a separate calculation is required. A remark should be made, that the vectors $\tilde{\boldsymbol{t}}_j(\boldsymbol{f})$ of (6) are close to the vectors $\bar{\boldsymbol{t}}_j(\boldsymbol{f})$ of (7), due to a typically good alignment between the tangent vectors $\boldsymbol{t}_j(\boldsymbol{f})$ and the eigenvectors $\boldsymbol{a}_j$, $j = 1, \ldots, N$.

Let us now address the issue of an appropriate choice of the number $K$ of the principal components. As mentioned before, one needs $K > N$. At the same time, the eigenvalues are normally quickly decreasing, which indicates that the majority of information about antenna response variability is contained within the subspace spanned by the first few eigenvectors. In practice, it suffices to appoint $K = N + 1$ or $N + 2$. The actual choice of $K$ is problem specific and will further be discussed in Section III.

In the last step, the first-level surrogate $\boldsymbol{s}_I(\boldsymbol{f})$ and the vectors $\boldsymbol{w}_j$ are used to defined the surrogate model domain $X_S$.
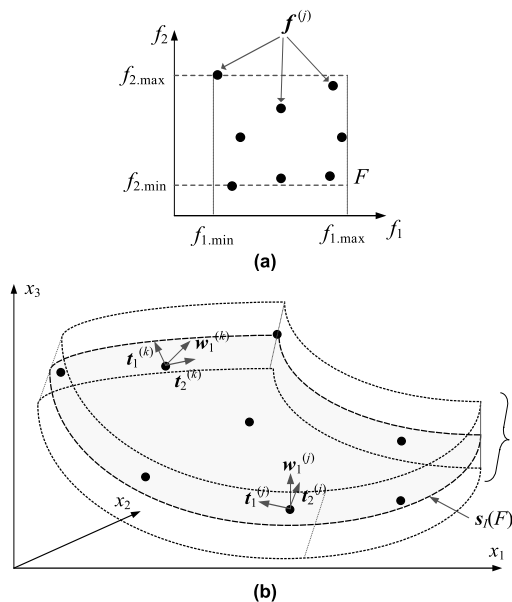
**FIGURE 1.** Conceptual illustration of the surrogate domain confinement with explicit dimensionality reduction: (a) two-dimensional objective space $F$, (b) three-dimensional parameter space $X$, the first-level model image $s_I(F)$, along with two exemplary points $s_I(f)$ and their respective tangent vectors $t_1$ and $t_2$ as well as the normal vector $w_1$; the reference designs are marked with black circles. It should be noted, that $K < n$, i.e., the intended dimensionality of the confined domain $X_S$ should be smaller than the dimensionality of the original parameter space $X$; yet, shown is the sole case that could be presented graphically, i.e., $K = n$.

We have

$$X_S = \left\{ \begin{array}{l} x = s_I(f) + T \sum_{k=1}^{K-N} \lambda_k w_n^{(k)}(f) : f \in F, \\ -1 \leq \lambda_k \leq 1, \ k = 1, \dots, n - N \end{array} \right\} \quad (9)$$

In other words, $X_S$ contained all points of the form

$$x = s_I(f) + T \sum_{k=1}^{K-N} \lambda_k w_n^{(k)}(f) \quad (10)$$

for all $f \in F$, and all combinations of $-1 \leq \lambda_k \leq 1$ for $k = 1, \dots, K - N$. The parameter $T$ of (9) refers to the lateral dimension of the domain $X_S$ and its value is chosen to be a fraction (between five and ten percent) of the reference set spread along the most dominant eigenvector. Also, it accommodates the relationships between the subsequent eigenvalues $\lambda_k$. A modification to this scheme is possible, in which individual coefficient values $T_k$ are adopted for each vector $w_k$, instead of a joint value $T$. This would enable to account for the relative contribution of particular directions and will be considered in the future work. The surrogate model domain dimensionality is appointed by selecting the parameter $K$. A graphical illustration of the considered concepts can be found in Fig. 1, here, presented for a two-dimensional objective space $F$, and a three-dimensional parameter space $X$. Figure 1 shows the case for the dimensionality $K$ of the domain $X_S$ equal to the dimensionality $n$ of $X$ (for enabling proper illustration). Whereas in practice one should assume $K < n$.

## B. RESPONSE FEATURES

The concept of handling appropriately chosen characteristic points (features) of the response of device at hand rather than its entire responses (e.g., frequency characteristics) has been successfully employed in antenna design in various contexts, such as modeling [52], parametric optimization [53] or statistical analysis [54]. The motivation behind reformulating the design task in terms of the response features has come from the scrutiny of the dependence of the feature coordinates on the design variables, which appears to be much less nonlinear (in fact, often close to linear) than a similar dependence of the original responses (see Fig. 2). Figure 2 provides graphical illustration of the benefits coming from employing response feature approach: the dependence of the feature point coordinates on the antenna parameters is shown in Figs. 2(b) and (c)), whereas the respective dependence for the entire characteristics is shown in Fig. 2(a).

Technically, the features have to be selected within a given design context and have to reflect the design goals. The actual selection of the response features requires the analysis of the system outputs and identification easily distinguishable characteristic points. The extraction of the response features from the EM simulations is carried out through post-processing.

An illustrative example of the concepts outlined above constitute narrow- and multi-band antennas. Here, a natural choice of response features are the points corresponding to the antenna resonances and −10 dB level of reflection. This selection of response features allows handling design tasks such as allocation of the resonances at the intended frequencies or enhancing the antenna bandwidth. It should be emphasized, that the feature-based approach allows for directly encoding the knowledge about the figures of interest relevant to the particular design optimization problem at hand. Whereas in the conventional approach, in which the entire responses are processed, subsequent extraction of this information is necessary.

The following notation will be used. Let $R(x)$ denote the EM-simulated antenna response at the design $x$. The symbol $R$ stands for the aggregated antenna outputs and may consists of its reflection response $S_{11}(x,f)$, gain $G(x,f)$, etc., where $f$ is the frequency within a certain simulation range as provided by the model. Let also $\varphi = [\varphi_1^T \ \dots \ \varphi_P^T]^T$ be the vector whose entries are the characteristic points of the response (features): $\varphi_k = [\omega_k \ \lambda_k]^T$, $k = 1, \dots, P$; with $\omega_k$ and $\lambda_k$ being the frequency and the level (magnitude) coordinates, respectively.

Let us recall the design task of matching improvement of multi-band antennas of Section II.A (cf. (2)). Here, the feature vector $\varphi$ comprises the frequency and level coordinates of the antenna resonances: $\omega_k = f_{0.k}$ and $\lambda_k = S_{11}(f_{0.k})$, $k = 1, \dots, P$, respectively. We have $\varphi = [\varphi_1^T \ \dots \ \varphi_P^T]^T = [f_{0.1} \ S_{11}(f_{0.k}) \ \dots \ f_{0.P} \ S_{11}(f_{0.P})]^T$, where $P$ refers to the number of antenna bands. In the case of bandwidth enhancement, the feature vector is $\varphi = [\varphi_1^T \ \dots \ \varphi_P^T]^T$, where each consecutive vector $\varphi_k^T = [f_{0.k} \ S_{11}(f_{0.k}) \ f_{L.k} \ S_{11}(f_{L.k}) \ f_{H.k} \ S_{11}(f_{H.k})]^T$, i.e., it contains the frequency and level coordinates of the $k$-th
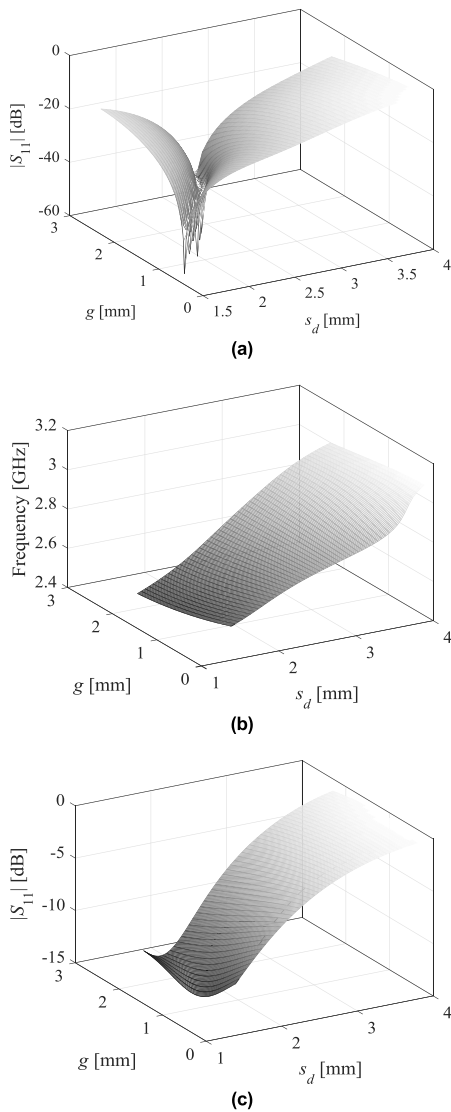
**FIGURE 2.** Graphical illustration of the benefits of response feature approach: (a) reflection responses of the ring slot antenna of Section 3 evaluated for $1.5 \leq s_d \leq 4.0$ and for $0.3 \leq g \leq 2.3$ at $f = 2.4$ GHz. Other geometry parameters are set to: $l_f = 27$, $l_d = 6.5$, $w_d = 2.2$, $r = 14.5$, $s = 5.3$, $o = 5.1$ (all dimensions in mm). The feature point components evaluated within the same design space region: frequency (b) and level (c). It can be observed that the dependence of the feature point coordinates on antenna geometry parameters is significantly less nonlinear than for the entire characteristics. At the same time, the information carried by the feature points is sufficient for handling the design problems the points were defined for (here, the matching improvement task of (2)).

antenna resonance, along with the coordinates of the points of $-10$ dB level of the antenna response around it, i.e., $\lambda_{L.k} = |S_{11}(f_{L.k})| = -10$ dB and $\lambda_{H.k} = |S_{11}(f_{H.k})| = -10$ dB, $k = 1, \ldots, k$.

In the feature-based framework, the objective function (1) has to be reformulated in terms of the response features and will be denoted as $U_f(\boldsymbol{\varphi}(\boldsymbol{x}))$. Accordingly, the design task is transformed into

$$\boldsymbol{x}^* = \arg\min_{\boldsymbol{x}} U_\varphi (\boldsymbol{\varphi}(\boldsymbol{x})) \qquad (11)$$
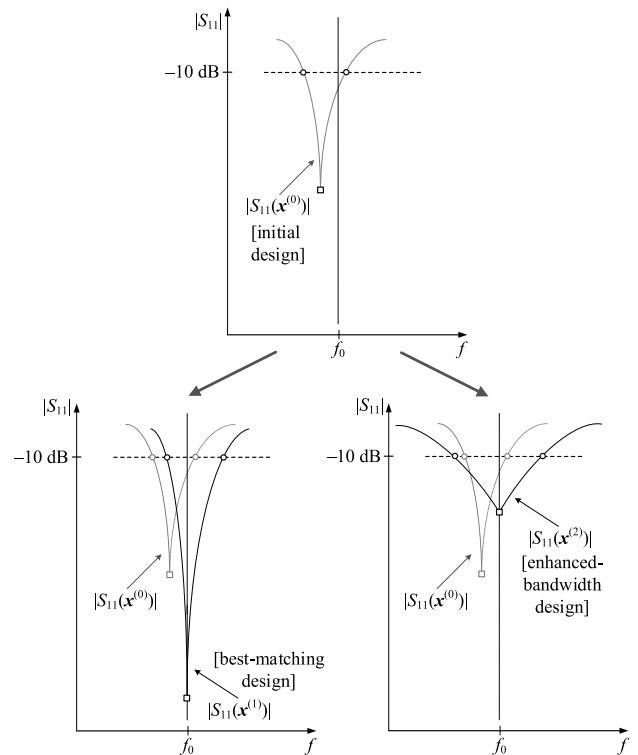


**FIGURE 3.** Graphical explanation of the response features selection for a particular design task: the features corresponding to $-10$ dB level (°) (for bandwidth enhancement at a target frequency $f_0$ – bottom-left panel), and the point corresponding to $f_0$ (□) (for antenna matching improvement at $f_0$ – bottom-right panel).

In the case of the multi-band antennas the merit function (2) of Section II.A may therefore be defined as

$$U_\varphi(\boldsymbol{x}, \boldsymbol{\varphi})$$
$$= \max \{|\lambda(\boldsymbol{x}, f_{0.1}(\boldsymbol{x}))|, \ldots, |\lambda(\boldsymbol{x}, f_{0.P}(\boldsymbol{x}))|\}$$
$$+ \beta \cdot || [f_{0.1}(\boldsymbol{x}) \ldots f_{0.P}(\boldsymbol{x})]^T - [f_{0.1}^t \ldots f_{0.P}^t]^T ||^2 \qquad (12)$$

where $f_{0.k}^t$ denotes the $k$-th target operating frequency, and $\beta$ is a penalty coefficient. In (12), the primary objective is minimization of antenna reflection, and the second term of (12) permits allocation of the antenna operating frequencies. In the case of bandwidth enhancement, the merit function may be defined as

$$U_\varphi(\boldsymbol{x}, \boldsymbol{\varphi}) = -\min \{B_1(\boldsymbol{x}), \ldots, B_P(\boldsymbol{x})\} \qquad (13)$$

where the $k$th relative (fractional) bandwidth is defined as

$$B_k(\boldsymbol{x}) = \frac{2 \cdot \min \{f_{0.k}(\boldsymbol{x}) - f_{L.k}(\boldsymbol{x}), f_{H.k}(\boldsymbol{x}) - f_{L.k}(\boldsymbol{x})\}}{f_{0.k}} \qquad (14)$$

The graphical illustration of the response features selection depending on the optimization goals is shown in Fig. 3. The top panel of Fig. 3 presents the exemplary antenna reflection characteristic at the initial design $\boldsymbol{x}^{(0)}$, along with the response features corresponding to the antenna resonance and $-10$ dB

reflection levels. The bottom-left panel of Fig. 3 shows the antenna response optimized for minimum in-band reflection with the use of the "resonance" feature point (marked with square). Whereas the bottom-right panel illustrates the response of the same structure optimized for maximum symmetrical bandwidth, obtained using the $-10$ dB characteristic points (marked with circles).

## C. PCA-BASED CONSTRAINED MODELING WITH RESPONSE FEATURES

The proposed feature-based modeling procedure over dimension-reduced constrained domain consists of the following steps:

1. Objective space $F$ definition by selecting relevant performance figures and their ranges;
2. Reference designs acquisition $x^{(j)}$, $j = 1, \ldots, p$, (Section II.A);
3. Application of the principal component analysis of the reference design set to yield the eigenvectors $a_k$ (Section II.A);
4. Construction of the first-level surrogate $s_I$;
5. Definition of the dimension-reduced constrained domain $X_S$ (Section II.A);
6. Allocation of the training data samples $x_B^{(k)}$, $k = 1, \ldots, N_B$, within $X_S$ (Section II.C);
7. Training data acquisition $R(x_B^{(k)})$, $k = 1, \ldots, N_B$;
8. Response features extraction $\varphi(R(x_B^{(k)}))$, $k = 1, \ldots, N_B$; (Section II.B);
9. Surrogate model identification based on the data pairs $\{x_B^{(k)}, \varphi(x_B^{(k)})\}_{k=1,\ldots,NB}$.

The surrogate model is set up within $X_S$ using kriging interpolation [55] with $\{x_B^{(k)}, \varphi(x_B^{(k)})\}_{k=1,\ldots,NB}$, being the training data set. The samples $x_B^{(k)}$ are uniformly allocated within $X_S$; $\varphi(x_B^{(k)})$ refer to the extracted characteristic points of the corresponding responses. The surrogate provides a prediction of the response feature coordinates for any given design $x$ within $X_S$. The details concerning the design experiments are delineated in the next subsection. Figure 4 shows the flow diagram of the overall modeling framework: exploiting the response feature technology outlined in Section II.B and operating on the constrained domain of reduced dimensionality (the domain definition with the use of the principal component analysis of the reference design set is described in Section II.A).

*Design of Experiments. Surrogate Model Optimization:* The geometry of the surrogate model domain is generally complex (in particular, its lateral dimensions significantly exceed the tangential ones), therefore, its handling may be inconvenient from the point of view of design of experiments (DoE). In particular, uniform allocation of the training data samples in $X_S$ is a nontrivial task. In order to facilitate DoE within the proposed framework, a surjective mapping $H$ between the unit hypercube $[0,1]^K$ (normalized domain) and $X_S$ is defined (see [47] for details). Using this transformation, it suffices to generate uniformly distributed data samples
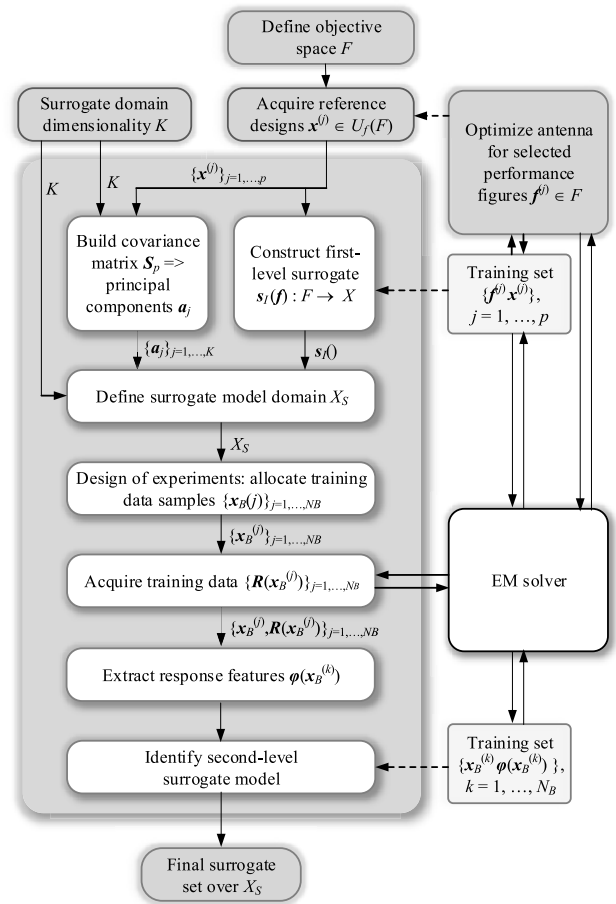


**FIGURE 4.** Flow diagram of the proposed surrogate modeling procedure exploiting the response feature technology and operating on the constrained domain of reduced dimensionality.

$\{z^{(k)}\}$, $k = 1, \ldots, N_B$, within $[0,1]^K$ using a standard procedure (e.g., Latin Hypercube Sampling [56]) and subsequently transform them into $X_S$ using $H$ as

$$x = H(z) = H([z_1 \ldots z_n]^T)$$
$$= s_I(f_z) + T \sum_{k=1}^{K-N} (-1 + 2z_{N+k})w_n^{(k)}(f_z) \quad (15)$$

where

$$f_z = [f_{1.\min} + z_1(f_{1.\max} - f_{1.\min}) \ldots f_{N.\min}$$
$$+ z_N(f_{N.\max} - f_{N.\min})]^T \quad (16)$$

The procedure (15), (16) is repeated for all vectors $z^{(k)}$ to yield the uniformly distributed training data set $\{x_B^{(k)}\}$ in $X_S$ as

$$x_B^{(k)} = H(z^{(k)}), \quad k = 1, \ldots, N_B \quad (17)$$

Note that the sample uniformity is understood with respect to the objective space $F$ rather than the domain $X_S$. For example, if the performance figure $f_1$ corresponds to the antenna center frequency $f_{0.1}$, the antenna designs are equally spread over the interval $[f_{1.\min}, f_{1.\max}]$.
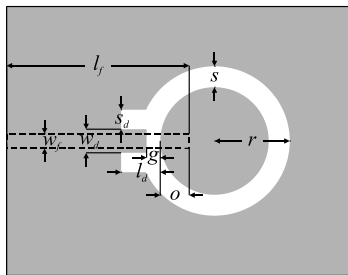
**FIGURE 5.** Geometry of Antenna I: ring slot antenna [50]; microstrip feed marked with dashed line.

In this work, similarly as in [40], the transformation H is also used to simplify the design optimization process. More specifically, the design task (11) can be transformed into an equivalent problem

$$\boldsymbol{x}^* = H(\boldsymbol{z}^*) \quad \text{where } \boldsymbol{z}^* = \arg\min_{\boldsymbol{z} \in [0,1]^n} U_\varphi\left(\boldsymbol{\varphi}(H(\boldsymbol{z}))\right) \qquad (18)$$

The benefit is that the problem (18) is solved over the normalized domain delimited by box constraints instead the geometrically complex set $X_S$. Possible formulations of the objective function $U_\varphi$ are given by (12) and (13)).

Furthermore, the first level surrogate can be employed to yield a quality initial design, which, for any given performance figure target vector $\boldsymbol{f}^t$ will be (for details, see [47])

$$\boldsymbol{x}^{(0)} = \boldsymbol{s}_I(\boldsymbol{f}^t) \qquad (19)$$

Given available data about the antenna at hand encoded in the reference design set, equation (19) produces the best possible approximation of the design optimum with respect to $\boldsymbol{f}^t$, which normally needs only a slight tuning by means of a local optimization algorithm.

## III. DEMONSTRATION CASE STUDIES

This section discusses validation of the modeling procedure outlined in Section 2, as well as provides comparisons with five benchmark procedures: the conventional data-driven surrogates: RBF (Model I), kriging interpolation (Model II), as well as three variants of the nested kriging technique: the basic procedure [47] (Model III), the feature-based version [49] (Model IV), as well as the dimensionally reduced nested kriging [48] (Model V). The numerical experiments involve three antennas: a ring-slot antenna, as well as a dual- and triple-band uniplanar dipoles. The application of the surrogates rendered within the proposed technique for antenna optimization is also investigated.

### A. CASE STUDY I: RING-SLOT ANTENNA

Our first example is a ring-slot antenna (Antenna I) depicted in Fig. 5 [57], implemented on a 0.76-mm-thick substrate. The substrate relative permittivity $\varepsilon_r$ is one of the two performance figures, the second being the antenna operating frequency. The antenna of Fig. 5 is fed through a microstrip line whose width $w_f$ is adjusted so that 50 ohm input impedance for the selected $\varepsilon_r$ value is ensured. The structure features

a circular ground plane slot with defected ground structure (DGS) for harmonic suppression [57]. The design variables are $\boldsymbol{x} = [l_f \; l_d \; w_d \; r \; s \; s_d \; o \; g]^T$. The antenna EM model $\boldsymbol{R}$ is simulated in CST ($\sim$300,000 cells, simulation time 90 s).

The surrogate is to cover the following ranges of the performance figures: operating frequency $f \in [2.5, 6.5]$ GHz and substrate permittivity $\varepsilon_r \in [2.0, 5.0]$. The lower and upper bounds on geometry parameters (derived based on the reference design set) are: $\boldsymbol{l} = [22.0 \; 3.5 \; 0.3 \; 6.5 \; 3.0 \; 0.5 \; 3.5 \; 0.2]^T$, and $\boldsymbol{u} = [27.0 \; 8.0 \; 2.3 \; 16.0 \; 7.0 \; 5.5 \; 6.0 \; 2.3]^T$, respectively. The database designs match the following pairs of $f$ and $\varepsilon_r$ (frequency in GHz): $\{f, \varepsilon_r\} = \{2.5 \, 2.0\}, \{4.5 \; 2.0\}, \{6.5 \; 2.0\}, \{2.5 \, 3.5\}, \{4.0 \, 3.5\}, \{5.0 \, 3.5\}, \{6.5 \, 3.5\}, \{2.5 \, 5.0\}, \{4.5 \, 5.0\},$ and $\{6.5 \; 5.0\}$.

The following setup for the validation process has been adopted. The surrogate models have been constructed within the proposed framework (Model VI) using the training data sets of various sizes: 20, 50, 100, 200, 400, and 800 samples. The modeling error (average relative RMS) has been estimated through the split sample method [58] with the test set consisting of 100 random samples.

The proposed procedure (Model VI) is benchmarked against the conventional models: RBF (Model I) and kriging (Model II), both set up within the unconstrained domain delimited by the lower and upper bounds on the parameters $\boldsymbol{l}$, $\boldsymbol{u}$, respectively. The benchmark methods also include the following performance-driven models built within the constrained domain: the original nested kriging (Model III), the version exploiting response features technology (Model IV), and dimensionality reduced nested kriging (Model V). The number of the principal directions $K = 4$ has been adopted for the proposed surrogate. This value has been assessed as the maximum justifiable value based on the analysis of the normalized eigenvalues of the reference designs: $\lambda_1 = 1.00$, $\lambda_2 = 0.09$, $\lambda_3 = 0.05$, $\lambda_4 = 0.026$, $\lambda_5 = 0.005$, $\lambda_6 = 0.004$, $\lambda_7 = 0.0005$, $\lambda_8 = 0.00005$.

The lateral dimension of the constrained domain $X_S$ has been set as $T = 0.5$ mm (this value corresponds to around 5 percent of the lateral span of the unconstrained domain $X$; see [47] for details). Table 1 gathers the results obtained for Antenna I within the proposed framework (Model VI) and all the benchmark procedures (Models I through V). It can be observed that all the surrogates constructed within constrained domains (Models III through VI) are considerably more reliable than those built within conventional interval-type domains (Models I and II), which are unusable for practical purposes even when set up with as many as 800 samples. Also, the proposed PCA- and feature-based surrogate (Model VI) is considerably more accurate than all other models rendered within any other variations of the nested kriging framework. It should also be observed that the feature-based frameworks (without dimensionality reduction (Model IV) and dimensionally reduced (Model VI)) allow for achieving practically acceptable predictive power even for the smallest data set sizes of as little as 20 or 50 samples.
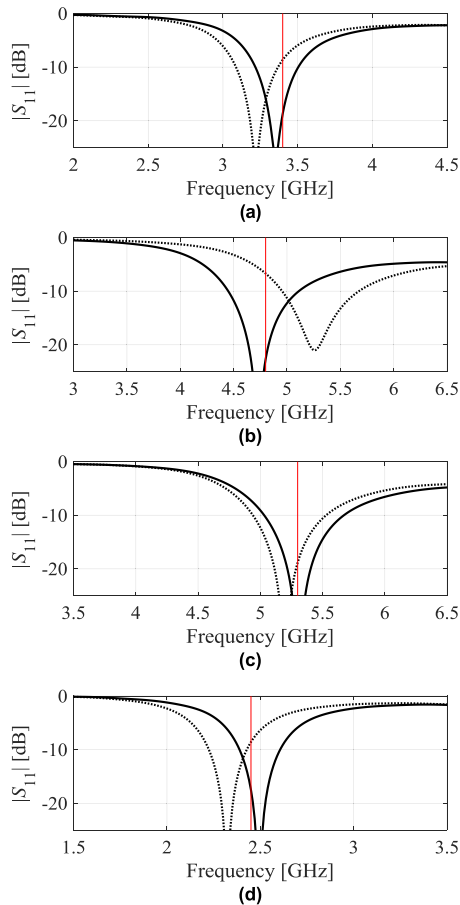
**FIGURE 6.** EM-simulated antenna responses of Antenna I: initial designs (·····) yielded by the proposed PCA-and feature-based surrogate, and the optimized designs (—). The designs obtained for the following objective vectors: (a) $f_0 = 3.4$ GHz, $\varepsilon_r = 3.5$, (b) $f_0 = 4.8$ GHz, $\varepsilon_r = 2.2$, (c) $f_0 = 5.3$ GHz, $\varepsilon_r = 3.5$, (d) $f_0 = 2.45$ GHz, $\varepsilon_r = 4.3$. Target operating frequencies are marked using vertical lines.

The design utility of the proposed modeling technique has been verified by employing the surrogate built for $K = 4$ and $N = 100$ training samples for parameter tuning of Antenna I. The numerical results for several target pairs of the performance figures (antenna operating frequency and substrate permittivity) are gathered in Table 2. Figure 6 presents EM-simulated responses of Antenna I: (i) the initial designs rendered by the proposed surrogate, as well as (ii) the optimized designs for the selected target operating vectors. The results presented in Fig. 6 corroborate that neither PCA-based dimensionality reduction of the constrained domain nor restricting the modeling process to response features rather than the entire antenna characteristics exert detrimental effects on the design quality. Thus, the proposed surrogate can be employed for antenna designing purposes: the optimized designs are of high quality and the operating frequencies are allocated with sufficient precision with respect to the target.

## B. CASE STUDY II: DUAL-BAND UNIPLANAR ANTENNA
The proposed modeling methodology has also been demonstrated using a dual-band antenna fed by a coplanar

**TABLE 1.** Modeling results and benchmarking for antenna I.

| Number of training samples | Relative RMS Error | | | | | |
|---|---|---|---|---|---|---|
| | Conventional Models | | Nested Kriging Model [47] | Nested Kriging Model with Response Features [49] | PCA-Based Nested Kriging Modeling [48] | PCA-Based Nested Kriging Modeling with Response Features [this work] |
| | Kriging | RBF | | | | |
| Model | I | II | III | IV | V | VI |
| 20 | 60.8 % | 64.5 % | 50.7 % | 5.3 % | 38.8 % | 2.52 % |
| 50 | 56.9 % | 61.0 % | 19.4 % | 4.7 % | 12.6 % | 0.90 % |
| 100 | 50.8 % | 53.2 % | 12.9 % | 2.8 % | 7.1 % | 0.18 % |
| 200 | 35.8 % | 37.9 % | 7.7 % | 2.5 % | 3.8 % | 0.15 % |
| 400 | 31.5 % | 34.1 % | 5.1 % | 2.3 % | 2.3 % | 0.25 % |
| 800 | 25.6 % | 27.2 % | 3.7 % | 2.0 % | 1.8 % | 0.20 % |

**TABLE 2.** Optimization results for antenna I.

| Target Operating Conditions | | Geometry Parameter Values [mm] | | | | | | | |
|---|---|---|---|---|---|---|---|---|---|
| $f_0$ [GHz] | $\varepsilon_r$ | $l_f$ | $l_d$ | $w_d$ | $r$ | $s$ | $s_d$ | $o$ | $g$ |
| 3.4 | 3.5 | 26.75 | 5.96 | 1.16 | 11.87 | 5.04 | 3.17 | 4.84 | 0.98 |
| 4.8 | 2.2 | 22.06 | 4.83 | 0.32 | 10.19 | 3.35 | 4.67 | 5.96 | 1.38 |
| 5.3 | 3.5 | 22.22 | 4.69 | 0.38 | 8.77 | 3.36 | 5.33 | 5.89 | 1.80 |
| 2.45 | 4.3 | 26.97 | 6.33 | 2.07 | 14.17 | 4.99 | 1.92 | 4.84 | 0.49 |

waveguide (Antenna II) shown in Fig. 7 [58]. The antenna structure is implemented on the RO4350 substrate with $\varepsilon_r = 3.48$, $h = 0.762$ mm. In Fig. 7, the designable parameter vector is $\boldsymbol{x} = [l_1\ l_2\ l_3\ w_1\ w_2\ w_3]^T$; with the following fixed dimensions: $l_0 = 30$, $w_0 = 3$, $s_0 = 0.15$ and $o = 5$ (all dimensions in mm). The computational model is simulated using CST Microwave Studio time-domain solver ($\sim$100,000 cells; simulation time $\sim$60 seconds).

In this case study, the surrogate model is to cover the following ranges of the antenna operating frequencies: $f_1 \in$ [2.0, 3.0] GHz (lower band) and $f_2 \in$ [4.0, 5.5] GHz (upper band). The reference designs of [40] were utilized, which correspond to the following pairs of the target operating frequencies: $\{f_1, f_2\}$ [GHz]: {2.0, 4.0}, {2.2, 5.0}, {2.0, 5.5}, {2.3, 4.5}, {2.4, 5.5}, {2.6, 4.0}, {2.7, 3.5}, {2.8, 4.7}, {3.0, 4.0}, and {3.0, 3.5}. The lower and upper bounds on geometry parameters are $\boldsymbol{l} = [29\ 5.0\ 17\ 0.2\ 1.5\ 0.5]^T$ and $\boldsymbol{u} = [42\ 12\ 25\ 0.6\ 5.2\ 3.5]^T$, respectively.

As in the previous case, the surrogates have been set up with the use of the training data sets of the sizes from 20 to 800 samples. The number of the principal directions has been set to $K = 4$, and the value of the extension parameter was $T = 0.25$ mm. The rationale behind this setup is similar to that of the first case study. Table 3 shows the modeling results for the benchmark methods (Models I through V), and the proposed one (Model VI).
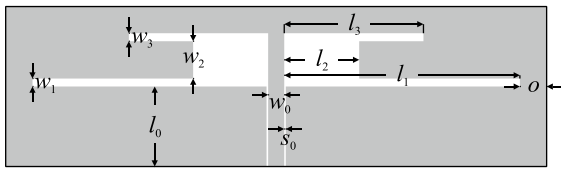
**FIGURE 7.** Geometry of Antenna II: uniplanar dual-band dipole antenna [52].

**TABLE 3.** Modeling results and benchmarking for antenna II.

| Number of training samples | Relative RMS Error | | | | | |
| | Conventional Models | | Nested Kriging Model [47] | Nested Kriging Model with Response Features [49] | PCA-Based Nested Kriging Modeling [48] | PCA-Based Nested Kriging Modeling with Response Features [this work] |
| | Kriging | RBF | | | | |
| Model | I | II | III | IV | V | VI |
| 20 | 24.5 % | 26.3% | 19.0 % | 1.43% | 10.0 % | 0.58 % |
| 50 | 21.7 % | 24.9 % | 9.9 % | 0.51% | 5.1 % | 0.29 % |
| 100 | 17.3 % | 19.8 % | 6.4 % | 0.39% | 2.9 % | 0.18 % |
| 200 | 12.6 % | 14.3 % | 4.4 % | 0.56% | 2.8 % | 0.21 % |
| 400 | 9.3 % | 10.5 % | 3.8 % | 0.43% | 2.1 % | 0.18 % |
| 800 | 7.2 % | 8.7 % | 3.4 % | 0.46% | 1.9 % | 0.14 % |

**TABLE 4.** Optimization results for antenna II.

| Target Operating Conditions | | Geometry Parameter Values [mm] | | | | | |
| $f_1$ [GHz] | $f_2$ [GHz] | $l_1$ | $l_2$ | $l_3$ | $w_1$ | $w_2$ | $w_3$ |
| 2.45 | 5.30 | 33.45 | 9.08 | 18.10 | 0.30 | 2.41 | 2.22 |
| 2.20 | 4.50 | 35.04 | 6.73 | 18.81 | 0.49 | 4.04 | 1.86 |
| 3.00 | 5.00 | 29.16 | 10.14 | 19.85 | 0.38 | 2.83 | 0.96 |
| 2.10 | 4.20 | 36.12 | 6.51 | 19.85 | 0.51 | 4.41 | 1.95 |

For supplemental verification, the proposed surrogate has been utilized for antenna optimization. Figure 8 and Table 4 show the results obtained with the surrogate built with 50 training samples for four different pairs of the target operating frequencies. Figure 8 shows EM-simulated initial and optimized responses of Antenna II. As in the previous example, the results of Fig. 8 confirm that PCA-based domain dimensionality reduction in conjunction with restricting the modeling process to response features are not detrimental to the quality of the optimal designs. As it stems from Fig. 8, even though the operating frequencies at the initial designs rendered by the first-level (inverse) surrogate for the assumed target vector are not allocated perfectly, the quality of the optimal designs is high and the design specifications are met.

## C. CASE STUDY III: TRIPLE-BAND UNIPLANAR ANTENNA

Our last example is a triple-band uniplanar antenna built as a stack of three ground plane slits separated by two slots
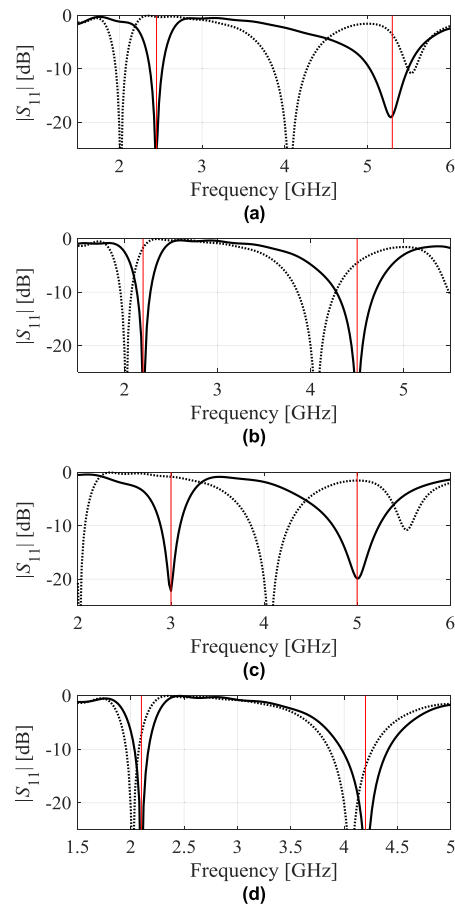


**FIGURE 8.** EM-simulated antenna responses of Antenna II: initial designs (.....) yielded by the proposed PCA-and feature-based surrogate, and the optimized designs (—). Vertical lines mark target operating frequencies: (a) $f_1 = 2.45$ GHz, $f_2 = 5.3$ GHz, (b) $f_1 = 2.2$ GHz, $f_2 = 4.5$ GHz, (c) $f_1 = 3.0$ GHz, $f_2 = 5.0$ GHz, and (d) $f_1 = 2.1$ GHz, $f_2 = 4.2$ GHz.
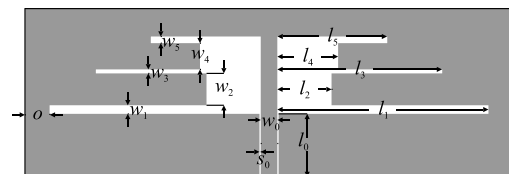


**FIGURE 9.** Geometry of antenna iii: uniplanar triple-band antenna [52].

that is fed by a coplanar waveguide [59]. Figure 9 shows the antenna geometry described by the following vector of the design variables: $\boldsymbol{x} = [l_1\ l_2\ l_3\ l_4\ l_5\ w_1\ w_2\ w_3\ w_4\ w_5]^T$; with $l_0 = 30$, $w_0 = 3$, $s_0 = 0.15$ and $o = 5$ being fixed (all dimensions in mm). As in the second case study, the structure is implemented on the RO4350 substrate. The numerical experiments are arranged similarly as in the first two examples: the training data sets sizes range from 20 to 800, the number of taken into account principal directions is $K = 4$, the extension parameter $T = 0.25$ mm. The antenna computational model is simulated using CST Microwave Studio transient solver ($\sim$180,000 cells; simulation time $\sim$80 seconds).

**TABLE 5.** Modeling results and benchmarking for Antenna III.

| Number of training samples | Conventional Models | | Nested Kriging Model [47] | Nested Kriging Model with Response Features [49] | PCA-Based Nested Kriging Modeling [48] | PCA-Based Nested Kriging Modeling with Response Features [this work] |
|---|---|---|---|---|---|---|
| | Relative RMS Error | | | | | |
| | Kriging | RBF | | | | |
| Model | I | II | III | IV | V | VI |
| 20 | 28.5 % | 30.1 % | 38.9 % | 2.65 % | 44.8 % | 1.71 % |
| 50 | 22.7 % | 23.5 % | 16.0 % | 0.25 % | 16.5 % | 0.66 % |
| 100 | 19.9 % | 19.8 % | 11.2 % | 0.22 % | 10.9 % | 0.24 % |
| 200 | 18.6 % | 19.2 % | 9.9 % | 0.19 % | 8.7 % | 0.89 % |
| 400 | 17.2 % | 18.8 % | 9.7 % | 0.14 % | 6.4 % | 0.43 % |
| 800 | 16.8 % | 17.4 % | 7.8 % | 0.20 % | 4.3 % | 0.19 % |

**TABLE 6.** Optimization results for Antenna III.

| Target Operating Frequencies [GHz] | | | Geometry Parameters [mm] | | | | | | | | | |
|---|---|---|---|---|---|---|---|---|---|---|---|---|
| $f_1$ | $f_2$ | $f_3$ | $l_1$ | $l_2$ | $l_3$ | $l_4$ | $l_5$ | $w_1$ | $w_2$ | $w_3$ | $w_4$ | $w_5$ |
| 1.6 | 2.56 | 3.58 | 40.20 | 4.85 | 33.89 | 9.63 | 24.66 | 0.25 | 0.95 | 0.78 | 2.43 | 0.61 |
| 1.8 | 2.34 | 3.51 | 39.05 | 7.98 | 34.08 | 7.80 | 24.67 | 0.43 | 1.23 | 0.49 | 2.37 | 0.82 |
| 2.1 | 2.94 | 4.12 | 37.24 | 9.98 | 31.24 | 10.32 | 22.58 | 0.50 | 1.29 | 0.91 | 1.09 | 0.55 |
| 2.4 | 3.36 | 5.04 | 36.42 | 12.08 | 29.03 | 11.21 | 20.48 | 0.57 | 0.94 | 1.04 | 0.59 | 0.67 |

For this case study, the goal is to build the surrogate valid for the antenna operating frequencies $f_k$, $k = 1, 2, 3$, with $f_2 = f_1 k_1$ and $f_3 = f_2 k_2$ (the actual operating frequencies are calculated based on the values of the ratios $k_1$ and $k_2$). The intended frequency ranges are: $f_1 \in [1.5, 2.5]$ GHz, and $k_1$, $k_2 \in [1.2, 1.6]$. For Antenna III, the objective space comprises the vectors $[f_1 \ k_1 \ k_2]^T$. The geometry parameter lower and upper bounds are: $l = [30 \ 5.0 \ 20 \ 5.0 \ 15 \ 0.2 \ 0.2 \ 0.2 \ 0.2 \ 0.2]^T$, and $u = [50 \ 15 \ 30 \ 15 \ 21 \ 2.2 \ 4.2 \ 2.2 \ 4.2 \ 2.2]^T$, respectively. Table 5 gathers the modelling errors for the proposed and benchmark frameworks.

As in the previous cases, the design utility of the proposed surrogate has been demonstrated by applying the model for antenna optimization. The results obtained by the surrogate constructed using 50 training samples for four different sets of the target operating frequencies are provided in Figure 10 and Table 6. Figure 10 presents the EM-simulated initial and optimized responses of Antenna III. The results corroborate suitability of the proposed both PCA- and feature-based modeling framework for antenna design purposes. Despite using such a low number of training data samples, the surrogate yields the optimized designs of acceptable quality with the target operating frequencies allocates according to the design specifications, which is corroborated by the full-wave simulations. In this case, the operating frequencies of the
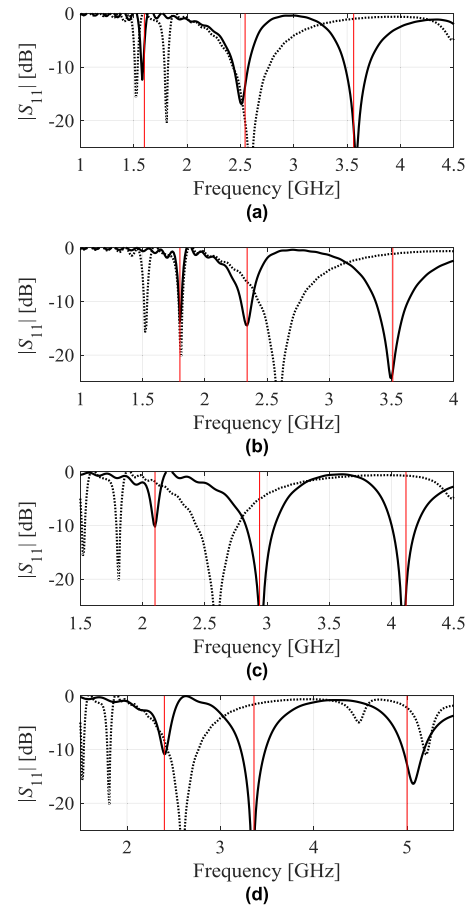


**FIGURE 10.** EM-simulated antenna responses of Antenna III: initial designs (.....) yielded by the proposed PCA-and feature-based surrogate, and the optimized designs (—). Vertical lines mark target operating frequencies: (a) $f_1 = 1.6$ GHz, $k_1 = 1.6$, $k_2 = 1.4$ ($f_2 = 2.56$ GHz, $f_3 = 3.58$ GHz), (b) $f_1 = 1.8$ GHz, $k_1 = 1.3$, $k_2 = 1.5$ ($f_2 = 2.34$ GHz, $f_3 = 3.51$ GHz), (c) $f_1 = 2.1$ GHz, $k_1 = 1.4$, $k_2 = 1.4$ ($f_2 = 2.94$ GHz, $f_3 = 4.12$ GHz), (d) $f_1 = 2.4$ GHz, $k_1 = 1.4$, $k_2 = 1.5$ ($f_2 = 3.36$ GHz, $f_3 = 5.04$ GHz).

initial designs are not accurately allocated, yet, the optimized designs meet the requirements.

## IV. CONCLUSION

The paper proposed a novel technique for reliable surrogate modelling of antenna structures. Our approach combines the nested kriging technique with explicit dimensionality reduction through principal component analysis with the response feature technology. Conducting the modelling process at the level of the feature points of the antenna responses while operating within the constrained domain of reduced dimensionality requires remarkably smaller training data sets—as compared to benchmark methods—to ensure usable predictive power of the surrogate. The formulation of the proposed technique incorporates the mechanisms for efficient design of experiments, and for expedited surrogate model optimization. Our methodology has been comprehensively validated based on the three microstrip antennas described by six to ten parameters. Thorough benchmarking against two conventional data-driven modeling techniques and three

variations of the performance-driven surrogates constructed within constrained domain corroborate reliability of our approach. Design utility of the proposed surrogate has been demonstrated through design optimization of the considered structures for various combinations of performance figures.

Admittedly, restricting the modelling process to selected characteristic points, rather than handling the entire responses, leads to a loss of information carried by the surrogate. Nevertheless, it allows for a dramatic reduction of the number of EM analyses required to secure usable accuracy of the model, therefore, it is highly desirable from the point of view of computational efficiency. At the same time, the information contained in the model is sufficient to employ it for design purposes, which is ensured by the appropriate definition of the characteristic points of the antenna responses. The technique presented in the paper can be viewed as an alternative to conventional modelling methods particularly in the situations when construction of low-cost surrogates for design tasks such as parameter tuning or dimension scaling is of interest. The primary application areas of the proposed framework would be a construction of re-usable models for rapid re-design of antenna structures (e.g., with respect to the operating frequencies and/or material parameters of the dielectric substrate), multi-objective optimization, expedited parameter tuning over broad ranges of operating conditions, as well as robust design. Furthermore, the technique can be applied to other classes of high-frequency structures, in particular, compact microwave components such as couplers, impedance matching transformers, or filters. In order to improve the versatility of the technique, the future work will be focused on the development of a generalized definition of response features that is less dependent on a particular structure of the antenna response, thereby allowing us to retain the consistency of the feature set across the parameter space. Generalization of this sort will enable utilization of the approach discussed in this work to a wider class of antenna systems.

## ACKNOWLEDGMENT

## REFERENCES

[1] Q. Liang, B. Sun, and G. Zhou, "Multiple beam parasitic array radiator antenna for 2.4 GHz WLAN applications," *IEEE Antennas Wireless Propag. Lett.*, vol. 17, no. 12, pp. 2513–2516, Dec. 2018.

[2] R. Rodriguez-Cano, S. Zhang, K. Zhao, and G. F. Pedersen, "Reduction of main beam-blockage in an integrated 5G array with a metal-frame antenna," *IEEE Trans. Antennas Propag.*, vol. 67, no. 5, pp. 3161–3170, May 2019.

[3] W. Lin and R. W. Ziolkowski, "Electrically small huygens CP rectenna with a driven loop element maximizes its wireless power transfer efficiency," *IEEE Trans. Antennas Propag.*, vol. 68, no. 1, pp. 540–545, Jan. 2020.

[4] T. Houret, L. Lizzi, F. Ferrero, C. Danchesi, and S. Boudaud, "DTC-enabled frequency-tunable inverted-F antenna for IoT applications," *IEEE Antennas Wireless Propag. Lett.*, vol. 19, no. 2, pp. 307–311, Feb. 2020.

[5] M. Virili, H. Rogier, F. Alimenti, P. Mezzanotte, and L. Roselli, "Wearable textile antenna magnetically coupled to flexible active electronic circuits," *IEEE Antennas Wireless Propag. Lett.*, vol. 13, pp. 209–212, 2014.

[6] J. Wang, M. Leach, E. G. Lim, Z. Wang, R. Pei, and Y. Huang, "An implantable and conformal antenna for wireless capsule endoscopy," *IEEE Antennas Wireless Propag. Lett.*, vol. 17, no. 7, pp. 1153–1157, Jul. 2018.

[7] G. P. Mishra and B. B. Mangaraj, "Miniaturised microstrip patch design based on highly capacitive defected ground structure with fractal boundary for X-band microwave communications," *IET Microw., Antennas Propag.*, vol. 13, no. 10, pp. 1593–1601, Aug. 2019.

[8] A. Meredov, K. Klionovski, and A. Shamim, "Screen-printed, flexible, parasitic beam-switching millimeter-wave antenna array for wearable applications," *IEEE Open J. Antennas Propag.*, vol. 1, pp. 2–10, 2020.

[9] J. L. Salazar-Cerreno, Z. Qamar, S. Saeedi, B. Weng, and H. S. Sigmarsson, "Frequency agile microstrip patch antenna using an anisotropic artificial dielectric layer (AADL): Modeling and design," *IEEE Access*, vol. 8, pp. 6398–6406, 2020.

[10] D. S. Prinsloo, A. Alayon Glazunov, R. Maaskant, M. V. Ivashina, V. Kukush, and P. Meyer, "Characterization and performance of an ultra-wideband wide-coverage multimode MIMO antenna," *IEEE Trans. Antennas Propag.*, vol. 67, no. 9, pp. 5812–5823, Sep. 2019.

[11] J.-F. Qian, F.-C. Chen, K.-R. Xiang, and Q.-X. Chu, "Resonator-loaded multi-band microstrip slot antennas with bidirectional radiation patterns," *IEEE Trans. Antennas Propag.*, vol. 67, no. 10, pp. 6661–6666, Oct. 2019.

[12] H. Sun and Z. Pan, "Design of a quad-polarization-agile antenna using a switchable impedance converter," *IEEE Antennas Wireless Propag. Lett.*, vol. 18, no. 2, pp. 269–273, Feb. 2019.

[13] F. D. C. B. de Sena and J. P. da Silva, "Harmonic suppression using optimised hexagonal defected ground structure by genetic algorithm," *IET Microw., Antennas Propag.*, vol. 12, no. 10, pp. 1645–1648, Aug. 2018.

[14] P. Kumar, S. Dwari, R. K. Saini, and M. K. Mandal, "Dual-band dual-sense polarization reconfigurable circularly polarized antenna," *IEEE Antennas Wireless Propag. Lett.*, vol. 18, no. 1, pp. 64–68, Jan. 2019.

[15] J. Zeng and K.-M. Luk, "Single-layered broadband magnetoelectric dipole antenna for new 5G application," *IEEE Antennas Wireless Propag. Lett.*, vol. 18, no. 5, pp. 911–915, May 2019.

[16] Z. Tang, X. Wu, J. Zhan, S. Hu, Z. Xi, and Y. Liu, "Compact UWB-MIMO antenna with high isolation and triple band-notched characteristics," *IEEE Access*, vol. 7, pp. 19856–19865, 2019.

[17] R. Lehmensiek and D. I. L. de Villiers, "Optimization of log-periodic dipole array antennas for wideband omnidirectional radiation," *IEEE Trans. Antennas Propag.*, vol. 63, no. 8, pp. 3714–3718, Aug. 2015.

[18] J. A. Easum, J. Nagar, P. L. Werner, and D. H. Werner, "Efficient multiobjective antenna optimization with tolerance analysis through the use of surrogate models," *IEEE Trans. Antennas Propag.*, vol. 66, no. 12, pp. 6706–6715, Dec. 2018.

[19] X. Du, L. Leifsson, and S. Koziel, "Rapid multi-band patch antenna yield estimation using polynomial chaos-kriging," in *Computational Science—ICCS* (Lecture Notes in Computer Science), vol. 11538, J. Rodrigues, Ed. Cham, Switzerland: Springer, 2019.

[20] L. A. Greda, A. Winterstein, D. L. Lemes, and M. V. T. Heckler, "Beam-steering and beamshaping using a linear antenna array based on particle swarm optimization," *IEEE Access*, vol. 7, pp. 141562–141573, 2019.

[21] Z. Medina, A. Reyna, M. A. Panduro, and O. Elizarraras, "Dual-band performance evaluation of time-modulated circular geometry array with microstrip-fed slot antennas," *IEEE Access*, vol. 7, pp. 28625–28634, 2019.

[22] A. Lalbakhsh, M. U. Afzal, and K. Esselle, "Simulation-driven particle swarm optimization of spatial phase shifters," in *Proc. Int. Conf. Electromagn. Adv. Appl. (ICEAA)*, Cairns, QLD, Australia, Sep. 2016, pp. 428–430.

[23] A. Lalbakhsh, M. U. Afzal, K. P. Esselle, and S. Smith, "Design of an artificial magnetic conductor surface using an evolutionary algorithm," in *Proc. Int. Conf. Electromagn. Adv. Appl. (ICEAA)*, Verona, Italy, Sep. 2017, pp. 885–887.

[24] A. Lalbakhsh, M. U. Afzal, K. P. Esselle, and S. L. Smith, "Wideband near-field correction of a Fabry–Perot resonator antenna," *IEEE Trans. Antennas Propag.*, vol. 67, no. 3, pp. 1975–1980, Mar. 2019.

[25] A. Lalbakhsh, M. U. Afzal, K. P. Esselle, and B. A. Zeb, "Multi-objective particle swarm optimization for the realization of a low profile bandpass frequency selective surface," in *Proc. Int. Symp. Antennas Propag. (ISAP)*, Hobart, TAS, Australia, 2015, pp. 1–4.

[26] J. S. Smith and M. E. Baginski, "Thin-wire antenna design using a novel branching scheme and genetic algorithm optimization," *IEEE Trans. Antennas Propag.*, vol. 67, no. 5, pp. 2934–2941, May 2019.

[27] S. M. Mikki, S. Clauzier, and Y. M. M. Antar, "Empirical geometrical bounds on MIMO antenna arrays for optimum diversity gain performance: An electromagnetic design approach," *IEEE Access*, vol. 6, pp. 39876–39894, 2018.

[28] S. Koziel and A. Pietrenko-Dabrowska, "Accelerated antenna optimization using gradient search with selective broyden updates," in *Proc. IEEE Int. Symp. Antennas Propag. USNC-URSI Radio Sci. Meeting*, Atlanta, GA, USA, Jul. 2019, pp. 1027–1028.

[29] J. A. Tomasson, S. Koziel, and A. Pietrenko-Dabrowska, "Expedited design closure of antenna input characteristics by trust region gradient search and principal component analysis," *IEEE Access*, vol. 8, pp. 8502–8511, 2020.

[30] M. M. T. Maghrabi, M. H. Bakr, S. Kumar, A. Z. Elsherbeni, and V. Demir, "FDTD-based adjoint sensitivity analysis of high-frequency nonlinear structures," *IEEE Trans. Antennas Propag.*, vol. 68, no. 6, pp. 4727–4737, Jun. 2020.

[31] I. A. Baratta, C. B. de Andrade, R. R. de Assis, and E. J. Silva, "Infinitesimal dipole model using space mapping optimization for antenna placement," *IEEE Antennas Wireless Propag. Lett.*, vol. 17, no. 1, pp. 17–20, Jan. 2018.

[32] S. Koziel and L. Leifsson, "Response correction techniques for surrogate-based design optimization of microwave structures," *Int. J. RF Microw. Comput.-Aided Eng.*, vol. 22, no. 2, pp. 211–223, Mar. 2012.

[33] S. Koziel and S. D. Unnsteinsson, "Expedited design closure of antennas by means of Trust-Region-Based adaptive response scaling," *IEEE Antennas Wireless Propag. Lett.*, vol. 17, no. 6, pp. 1099–1103, Jun. 2018.

[34] S. Koziel, Q. S. Cheng, and J. W. Bandler, "Feature-based surrogates for low-cost microwave modelling and optimisation," *IET Microw., Antennas Propag.*, vol. 9, no. 15, pp. 1706–1712, Dec. 2015.

[35] J. A. Easum, J. Nagar, and D. H. Werner, "Multi-objective surrogate-assisted optimization applied to patch antenna design," in *Proc. IEEE Int. Symp. Antennas Propag. USNC/URSI Nat. Radio Sci. Meeting*, San Diego, CA, USA, Jul. 2017, pp. 339–340.

[36] P. Barmuta, F. Ferranti, G. P. Gibiino, A. Lewandowski, and D. M. M.-P. Schreurs, "Compact behavioral models of nonlinear active devices using response surface methodology," *IEEE Trans. Microw. Theory Techn.*, vol. 63, no. 1, pp. 56–64, Jan. 2015.

[37] F. Feng, W. Zhang, J. Zhang, Z. Zhao, J. Jin, and Q. Zhang, "Recent advances in EM parametric modeling using combined neural network and transfer function," in *Proc. IEEE Int. Symp. Antennas Propag.*, Xi'an, China, 2019, pp. 1–3.

[38] M. Jamshidi, A. Lalbakhsh, S. Lotfi, H. Siahkamari, B. Mohamadzade, and J. Jalilian, "A neuro-based approach to designing a Wilkinson power divider," *Int. J. RF Microw. Comput.-Aided Eng.*, vol. 30, no. 3, Mar. 2020, Art. no. e22091.

[39] M. Jamshidi, A. Lalbakhsh, B. Mohamadzade, H. Siahkamari, and S. M. H. Mousavi, "A novel neural-based approach for design of microstrip filters," *AEU-Int. J. Electron. Commun.*, vol. 110, Oct. 2019, Art. no. 152847.

[40] J. P. Jacobs, "Characterisation by Gaussian processes of finite substrate size effects on gain patterns of microstrip antennas," *IET Microw., Antennas Propag.*, vol. 10, no. 11, pp. 1189–1195, Aug. 2016.

[41] D. R. Prado, J. A. Lopez-Fernandez, M. Arrebola, and G. Goussetis, "Support vector regression to accelerate design and crosspolar optimization of shaped-beam reflectarray antennas for space applications," *IEEE Trans. Antennas Propag.*, vol. 67, no. 3, pp. 1659–1668, Mar. 2019.

[42] D. Gorissen, K. Crombecq, I. Couckuyt, T. Dhaene, and P. Demeester, "A surrogate modeling and adaptive sampling toolbox for computer based design," *J. Mach. Learn. Res.*, vol. 11, pp. 2051–2055, Jul. 2010.

[43] S. N. Lophaven, H. B. Nielsen, and J. Søndergaard, "DACE: A MATLAB kriging toolbox," Univ. Denmark, Lyngby, Denmark, Tech. Rep. IMM-TR-2002-12, 2002.

[44] S. Marelli and B. Sudret, "UQLab: A framework for uncertainty quantification in MATLAB," in *Proc. Vulnerability, Uncertainty, Risk*, London, U.K., Jun. 2014, pp. 2554–2563.

[45] S. Koziel, "Low-cost data-driven surrogate modeling of antenna structures by constrained sampling," *IEEE Antennas Wireless Propag. Lett.*, vol. 16, pp. 461–464, 2017.

[46] S. Koziel and A. T. Sigurdsson, "Triangulation-based constrained surrogate modeling of antennas," *IEEE Trans. Antennas Propag.*, vol. 66, no. 8, pp. 4170–4179, Aug. 2018.

[47] S. Koziel and A. Pietrenko-Dabrowska, "Performance-based nested surrogate modeling of antenna input characteristics," *IEEE Trans. Antennas Propag.*, vol. 67, no. 5, pp. 2904–2912, May 2019.

[48] S. Koziel, A. Pietrenko-Dabrowska, and M. Al-Hasan, "Design-oriented two-stage surrogate modeling of miniaturized microstrip circuits with dimensionality reduction," *IEEE Access*, vol. 8, pp. 121744–121754, 2020.

[49] S. Koziel and A. Pietrenko-Dabrowska, "Design-oriented computationally-efficient feature-based surrogate modelling of multi-band antennas with nested kriging," *AEU-Int. J. Electron. Commun.*, vol. 120, Jun. 2020, Art. no. 153202.

[50] I. T. Jolliffe, *Principal Component Analysis*, 2nd ed. New York, NY, USA: Springer, 2002.

[51] D. Bau, III, and L. N. Trefethen, *Applied Numerical Linear Algebra*. Philadelphia, PA, USA: SIAM, 1997.

[52] S. Koziel, Q. S. Cheng, and J. W. Bandler, "Feature-based surrogates for low-cost microwave modelling and optimisation," *IET Microw., Antennas Propag.*, vol. 9, no. 15, pp. 1706–1712, Dec. 2015.

[53] S. Koziel and A. Pietrenko-Dabrowska, "Expedited feature-based quasi-global optimization of multi-band antenna input characteristics with jacobian variability tracking," *IEEE Access*, vol. 8, pp. 83907–83915, 2020.

[54] S. Koziel and J. W. Bandler, "Rapid yield estimation and optimization of microwave structures exploiting feature-based statistical analysis," *IEEE Trans. Microw. Theory Techn.*, vol. 63, no. 1, pp. 107–114, Jan. 2015.

[55] T. W. Simpson, J. D. Poplinski, P. N. Koch, and J. K. Allen, "Metamodels for computer-based engineering design: Survey and recommendations," *Eng. with Comput.*, vol. 17, no. 2, pp. 129–150, Jul. 2001.

[56] B. Beachkofski and R. Grandhi, "Improved distributed hypercube sampling," in *Proc. 43rd AIAA/ASME/ASCE/AHS/ASC Struct., Structural Dyn., Mater. Conf.*, Apr. 2002, p. 1274.

[57] C.-Y.-D. Sim, M.-H. Chang, and B.-Y. Chen, "Microstrip-fed ring slot antenna design with wideband harmonic suppression," *IEEE Trans. Antennas Propag.*, vol. 62, no. 9, pp. 4828–4832, Sep. 2014.

[58] P. Jiang, Q. Zhou, and X. Shao, "Verification methods for surrogate models," in *Surrogate Model-Based Engineering Design and Optimization* (Springer Tracts in Mechanical Engineering). Singapore: Springer, 2020, pp. 89–113.

[59] Y.-C. Chen, S.-Y. Chen, and P. Hsu, "Dual-band slot dipole antenna fed by a coplanar waveguide," in *Proc. IEEE Antennas Propag. Soc. Int. Symp.*, Jul. 2006, pp. 3589–3592.

**ANNA PIETRENKO-DABROWSKA** (Senior Member, IEEE) received the M.Sc. and Ph.D. degrees in electronic engineering from the Gdańsk University of Technology, Poland, in 1998 and 2007, respectively. She is currently an Associate Professor with the Gdańsk University of Technology, Poland. Her research interests include simulation-driven design, design optimization, control theory, modeling of microwave and antenna structures, and numerical analysis.

**SLAWOMIR KOZIEL** (Senior Member, IEEE) received the M.Sc. and Ph.D. degrees in electronic engineering from the Gdańsk University of Technology, Poland, in 1995 and 2000, respectively, the M.Sc. degrees in theoretical physics and in mathematics, in 2000 and 2002, respectively, and the Ph.D. degree in mathematics from the University of Gdańsk, Poland, in 2003. He is currently a Professor with the Department of Engineering, Reykjavik University, Iceland. His research interests include CAD and modeling of microwave and antenna structures, simulation-driven design, surrogate-based optimization, space mapping, circuit theory, analog signal processing, evolutionary computation, and numerical analysis.